

# Mechanism of Bond Zone Wave Formation in Explosion-Clad Metals

G. R. COWAN, O. R. BERGMANN, AND A. H. HOLTZMAN

Results of experiments in which the collision variables were carefully controlled showed that bond zone wave formation during explosion cladding is analogous to the formation of vortex streets in fluid flow around an obstacle or in the collision of liquid streams. The fluid flow analogy explains the observed transition from a smooth metal-to-metal bond zone to a wavy bond zone above a critical collision velocity. This model is capable of predicting the minimum collision velocity necessary for bond zone wave formation in different metal systems and it also predicts correctly the strong dependence of wave size on collision angle. The magnitude of the wave size agrees with that predicted from fluid flow past a flat plate. Two other mechanisms of bond zone wave formation were explored experimentally and found to be invalid.

**D**URING the last few years, explosion cladding of metals has become an established process for the production of a variety of clad metal products. The process was pioneered and is now used commercially by E. I. du Pont de Nemours & Co. The principles of the bonding mechanism and the different bond zone types found in explosion-clad metals were described by Cowan and Holtzman.<sup>1</sup> Further discussions of the process and extensive information on the properties and applications of explosion clads may be found in the recent literature.<sup>2-10</sup>

The important principles involved in explosion cladding of metals may be summarized as follows. During the high-velocity collision of metal plates, a high-velocity forward jet is formed between the metal plates if the collision angle and the collision velocity are in the range required for bonding, Fig. 1. The surface layers on the metals, containing nonmetallic films such as oxide films that are detrimental to the establishment of a metallurgical bond, are swept away in the jet. The metal plates themselves, cleaned of any surface films by the jet action, are joined at an internal point under the influence of the very high pressure that is obtained near the collision region. This high pressure also causes considerable local plastic deformation of the metals in the bond zone area. The bond is metallurgical in nature and usually as strong or stronger than the weaker parent metal. The actual existence of a jet in explosion cladding was experimentally confirmed recently by Bergmann, Cowan, and Holtzman<sup>11</sup> using two independent methods.

Explosion-clad metals very often show a wavy bond zone interface. Aside from its technological importance, the wavy bond is remarkable because of the very regular periodic pattern in which it appears, Fig. 2. This regularity is particularly surprising when the violent conditions of bond zone formation are considered. It was first proposed by Cowan and Holtzman<sup>1</sup> that the formation of bond zone waves in

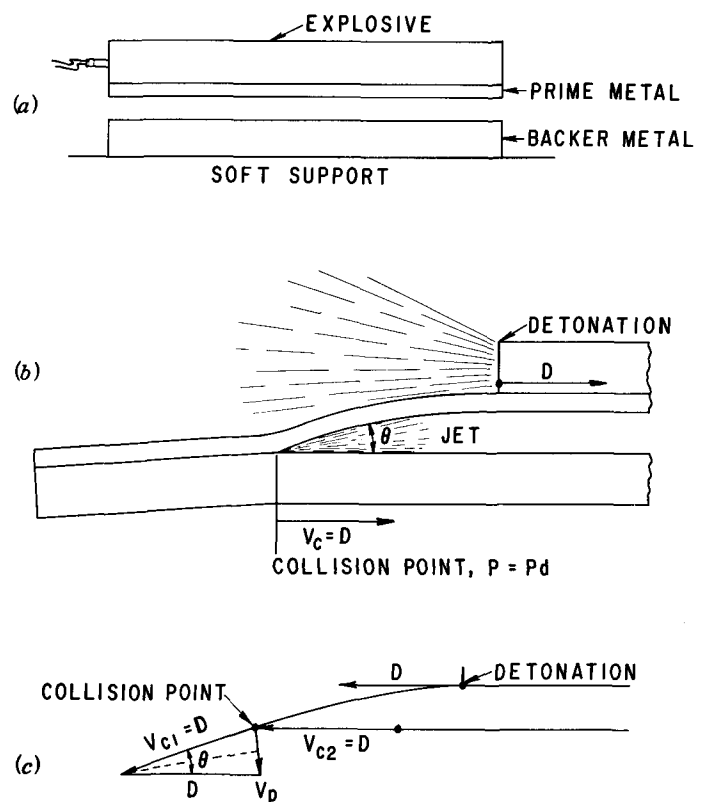


Fig. 1—(a) Typical cladding arrangement before detonation of the explosive. (b) Schematic drawing of the collision process. (c) Geometry of the steady-state collision.

explosion clads is analogous to fluid flow around an obstacle in which a regular formation of eddies is observed when the Reynolds number of the flow is above 50. In a subsequent paper, Klein<sup>12</sup> supported this view and showed that the ratio of the lateral distance between vortex streets and the longitudinal distance between vortex centers is essentially the same for typical wavy bond zones of explosion clads and for stable vortex streets in fluid flow. Burkhardt, Hornbogen, and Keller<sup>13</sup> observed transition from a smooth to a wavy bond zone above a critical collision velocity in angle clads. They also used the fluid flow analogy

G. R. COWAN and O. R. BERGMANN are Research Fellow and Manager of Technical Programs, Eastern Laboratory, E. I. du Pont de Nemours & Co., Gibbstown, N.J. A. H. HOLTZMAN is Manager of Research and Development, Explosive Products Division, Explosives Department, E. I. du Pont de Nemours & Co., Wilmington, Del.  
 Manuscript submitted December 16, 1968.

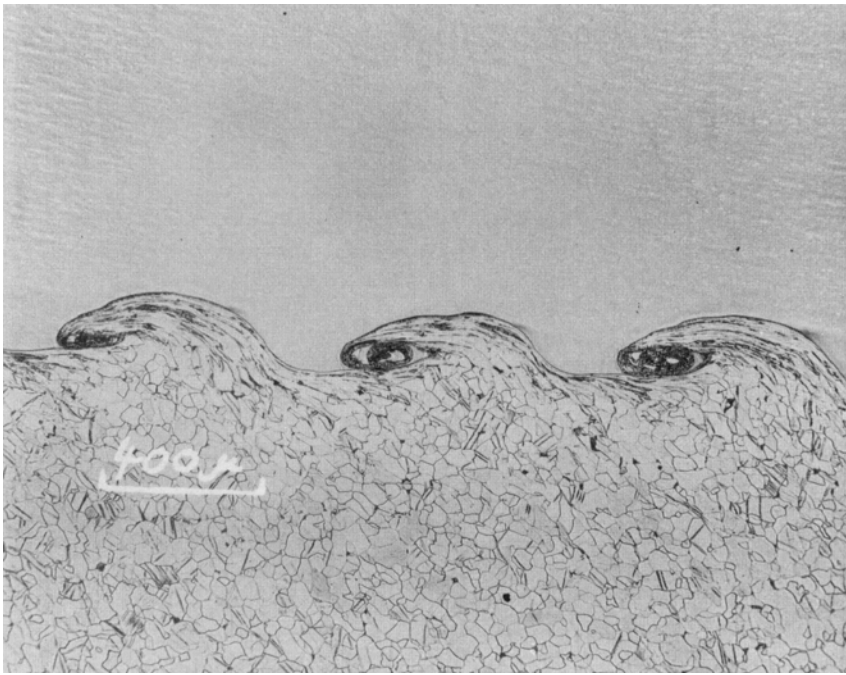


Fig. 2—Typical wavy bond zone—titanium on steel.

concept to explain the observed phenomena and attempted to derive a “Reynolds Number” for the observed transition from smooth to oscillating flow in the metals. However, they did not succeed in deriving a satisfactory expression capable of prediction. A pictorial description of bond zone wave formation during cladding was given by Bergmann.<sup>14</sup> Bahrani, Black, and Crossland<sup>15</sup> presented a more detailed pictorial description for an asymmetric system. The above-mentioned studies are qualitative in their description of the wave formation mechanism. It was highly desirable to study the wave formation mechanism in more quantitative terms capable of predicting the conditions required for wave formation as well as the factors controlling the size of the waves. The work described in this paper was aimed at providing a basis for such information. The fluid flow analogy as well as other mechanisms were explored and compared with experimental results.

#### THE WAVY BOND ZONE

The striking similarity between the wavy bond zone and von Karman vortex streets in fluid flow suggests that an examination of the known behavior of fluids<sup>16,17</sup> would provide guidance in developing an understanding of the factors that control the onset of the waviness and the size of the waves in cladding. However, two difficulties are encountered. There is no analytical solution for the flow equations describing the oscillating flow. (However, Harlow and Fromm<sup>18</sup> carried out complex numerical solutions to the Navier Stokes equations for a contrived flow similar to flow past an obstacle, and demonstrated the development of a vortex street above a critical Reynolds number.) It is, therefore, necessary to rely on analogy with experimental observations on vortex streets in fluids. Unfortunately the geometrically similar flow in fluids, *i.e.*, the collision of two flat liquid streams has not been studied. (As shown later we have con-

firmed experimentally that a transition from smooth to vortex flow does indeed occur with colliding liquid streams.) Therefore, we must base our analogy on the flow of fluids around obstacles, such as a transverse cylinder or a flat plate.

The second difficulty in the comparison is the difference between the deformational properties of metals and liquids. The finite yield strength of metals complicates their behavior and requires a suitable definition of the Reynolds number.

Before proceeding further, it is desirable to define the collision variables. The experiments reported here were all made using the parallel cladding technique used in commercial cladding operations. As shown in Fig. 1, the prime metal plate is initially parallel to and spaced away from the backer plate by a uniform stand-off. A uniform layer of explosive covering the prime metal plate is initiated at a point or line and the detonation, proceeding with a velocity  $D$  along the plate, drives it progressively into collision with the backer plate. Under these conditions a steady configuration is quickly attained in which the collision moves along the backer plate with a velocity  $V_c$  that equals  $D$ . The detonation products exert a pressure normal to the prime metal plate, with any shearing traction being negligible in comparison with the strength of the metal. Thus in the steady-state coordinate system moving with the collision, the magnitude of the velocity of the prime metal plate is not changed by the detonation, but the direction of the velocity is changed by an angle  $\theta$  equal to the collision angle. Both prime metal and backer plates are approaching the collision region with the same stream velocity or collision point velocity  $V_c$ . (Angle cladding, in which the prime metal plate is initially placed at an angle to the backer plate, has the added complication that the collision point velocities for the two plates are different.) It is clear from Fig. 1 that the relative plate velocity, *i.e.*, the velocity of the prime metal plate,  $V_p$ , just before collision is related to the collision

angle  $\theta$  by the expression

$$V_p = 2V_c \sin(\theta/2) \quad [1]$$

The jetting collision generates extremely high pressures; the peak pressure at the separation point at the base of the jet<sup>1</sup> slightly exceeds the stagnation pressure for an incompressible stream of density  $\rho$ ,

$$P_d = \rho V_c^2/2 \quad [2]$$

The collision pressure, typically a few hundred kilobars, thus exceeds the detonation pressure by a factor of about 10, and exceeds the residual pressure of the explosive products in the collision region still more. The resisting pressure of the relatively soft material of low impedance resisting the downward motion of the backer plate is also negligible compared to the collision pressure. Therefore, the collision process can be completely specified by the two collision variables  $V_c$  and  $\theta$  and the properties of the two plates, including the densities  $\rho_p$ ,  $\rho_b$  and the masses per unit area  $m_p$ ,  $m_b$ .

Because the very high pressure near the collision point greatly exceeds the yield strengths of the metals, the rate of plastic deformation near the collision point will be extremely high, and even when the metals do not melt their flow behavior will be liquid-like in the sense of being strain rate dependent and characterized by an effective viscosity. However, farther from the collision point the rate of deformation is much slower, and the behavior will be more influenced by the yield strength of the metal. It is of interest to consider the transition from smooth to oscillating flow for two ideal materials, a Newtonian liquid characterized by a constant viscosity, and an ideal elastic-plastic solid, characterized by a yield and constant flow stress.

The transition from a smooth to an oscillating wake in fluid flow past an obstacle occurs when a critical value of the Reynolds number is exceeded. The Reynolds number for the flow of a Newtonian liquid is defined as

$$R = dV_c\rho/\mu \quad [3]$$

where  $V_c$  is the upstream velocity relative to the obstacle,  $\mu$  is the viscosity and  $d$  is a characteristic dimension of the obstacle, *e.g.*, the diameter of a transverse cylinder. In the collision of two liquid streams the characteristic dimension may be taken as the thickness of the ideal jet in the absence of friction. As shown below the thickness of the ideal jet is proportion to  $\theta^2$ . Thus the boundary line for a critical value of the Reynolds number is defined by

$$\theta^2 V_c = a \text{ constant.} \quad [4]$$

For the ideal elastic plastic solid the critical Reynolds number must be defined in terms of the yield stress  $Y$ . Thus

$$R_e = \frac{dV_c\rho}{\mu} = \frac{(1/2)\rho V_c^2}{\mu V_c/2d} \propto \frac{P_d}{Y} \quad [5]$$

Thus the boundary line for oscillating flow is defined by

$$V_c = a \text{ constant} \quad [6]$$

The boundary line for wavy bond zones in cladding of metals may be expected to approximate a superposition

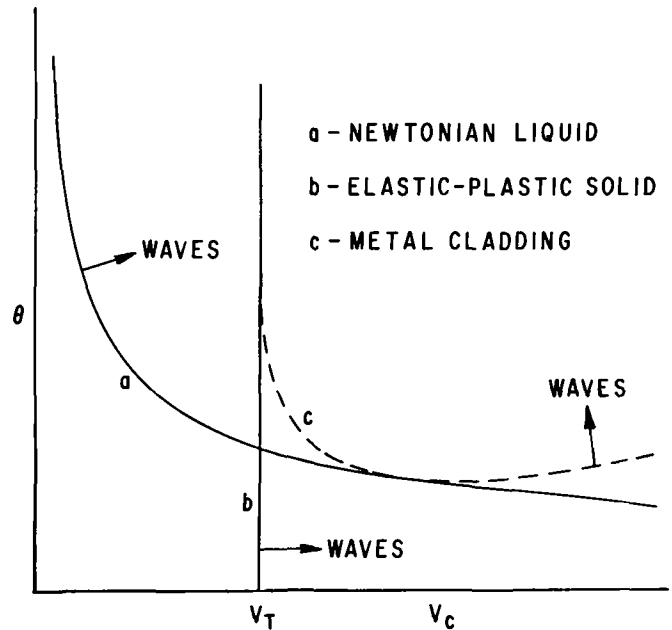


Fig. 3—Theoretical boundaries of wave formation for collisions (a) of flat streams of Newtonian liquids, and (b) of flat plates of elastic-plastic solids. (c) Typical observed boundary of wavy bond zones in metal cladding.

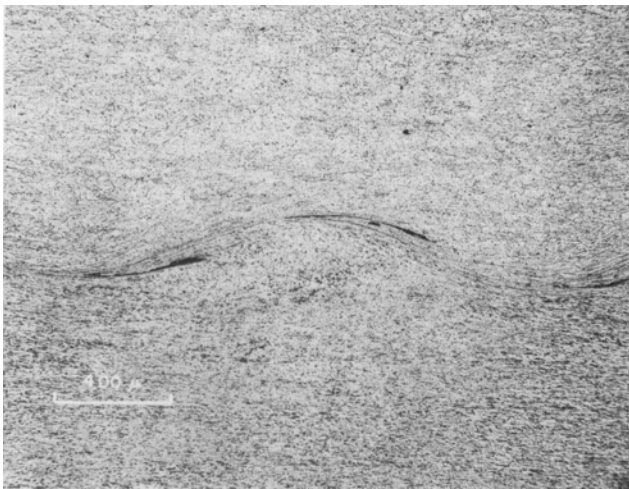
of these two ideal cases. This is indeed the case, as shown schematically by the dashed line in Fig. 3. The portion of the boundary at high values of  $V_c$  has not been well studied; the behavior there is undoubtedly complicated by melting and perhaps by the extremely high pressures at the separation point. This region is not of much practical interest because cladding is usually carried out at substantially higher values of  $\theta$  to ensure good bond quality in spite of variations in the collision variables associated with practical tolerances, *e.g.*, in flatness. In contrast the boundary line at higher values of  $\theta$  and low values of  $V_c$  is not only of practical interest, but also is of interest because of the possibility of relating it to the static strength of the metals. The objectives of this work are to account for the transition from a smooth to a wavy bond zone at relatively large values of the collision angle, and for the dependence of wave size on the collision velocity and angle.

## CLADDING EXPERIMENTS

The effect on the nature of the bond zone of varying the collision velocity is illustrated by the results obtained from a number of cladding experiments using the systems aluminum/aluminum, nickel/nickel and nickel/steel. As noted above, in the parallel cladding method used in these experiments, the collision velocity is equal to the detonation velocity, and was varied by selecting different types of explosive. The collision angle was kept constant at about 12 deg for all experiments by selecting values of explosive load and initial stand-off between the prime metal and backer. The required stand-off values were determined in separate experiments in which the acceleration of the prime metal plate by the detonation was observed in the absence of the backer plate. In all



(a)



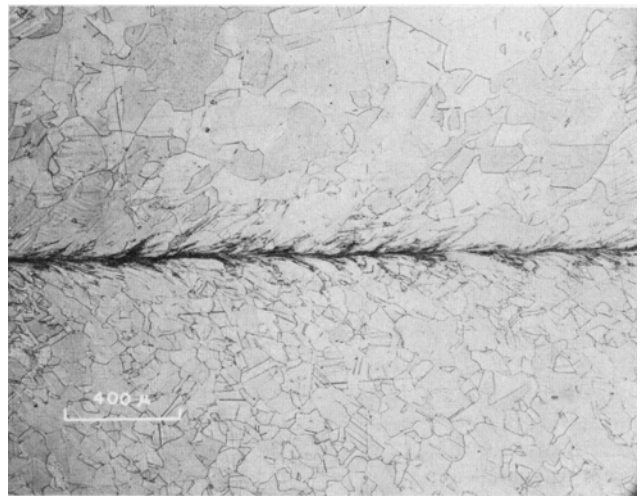
(b)



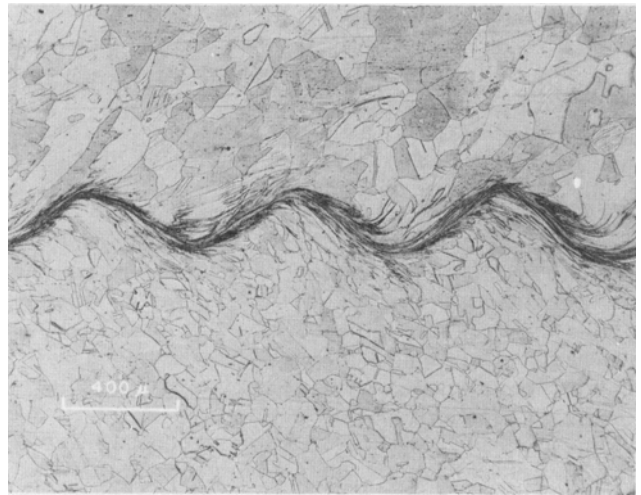
(c)

Fig. 4—Bond zones of aluminum-on-aluminum (Grade 1100H14) clads made at different collision velocities. (a)  $V_C = 1760$  m per sec; (b)  $V_C = 2020$  m per sec; (c)  $V_C = 2700$  m per sec.

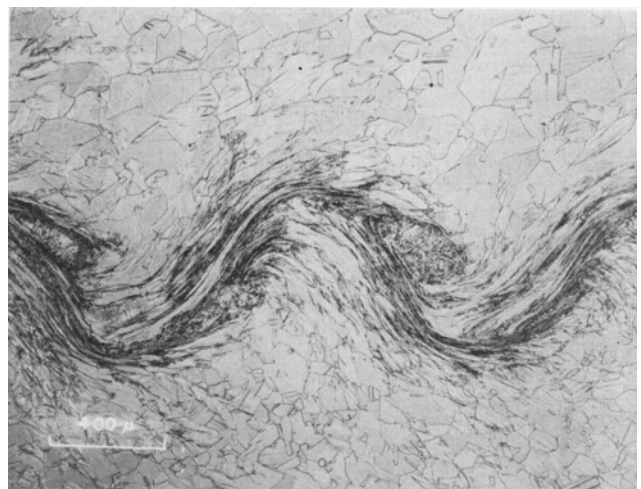
experiments reported here the detonation velocity was less than the minimum shock velocity of the metals, thus ensuring the absence of shock waves; the deflection angle of the prime plate is then a smooth



(a)



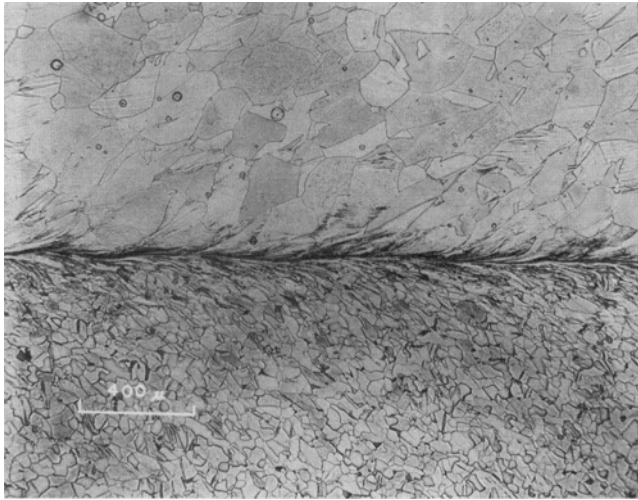
(b)



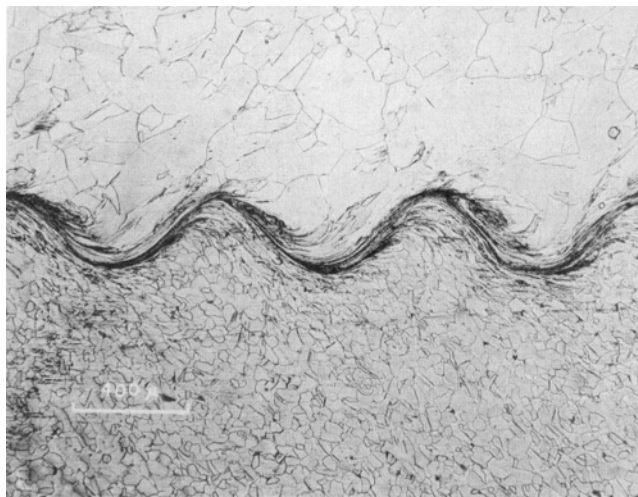
(c)

Fig. 5—Bond zones of nickel-on-nickel (Grade A) clads made at different collision velocities. (a)  $V_C = 1365$  m per sec; (b)  $V_C = 1790$  m per sec; (c)  $V_C = 2800$  m per sec.

function of the displacement across the stand-off gap. The angles were measured directly by an optical grid reflection technique with a high-speed framing camera. This method has been described by Cowan and



(a)



(b)



(c)

Fig. 6—Bond zones of nickel (Grade A) on steel (Grade 1008) clads made at different collision velocities. (a)  $V_c$  = approx 1600 m per sec; (b)  $V_c$  = 1900 m per sec; (c)  $V_c$  = approx 2500 m per sec.

Balchan.<sup>19</sup> After cladding, the bond zone character of each clad was determined metallographically, and the results are illustrated in Figs. 4, 5, and 6. It is seen that an essentially straight, smooth bond zone

is obtained at relatively low collision velocities. At higher collision velocities the bond zone becomes wavy. At still higher collision velocities pockets of solidified melt begin to appear in the eddy regions. The size of the melt pockets increases sharply with further increase in collision velocity.

A number of similar experiments were made with a number of different metal combinations in order to determine by bracketing the value of the collision velocity at the transition from a smooth to a wavy bond zone; these are listed in Table I.

Another set of experiments was made to explore the dependence of wave size on the collision variables. A number of  $\frac{1}{8}$ -in. nickel on  $\frac{1}{2}$ -in. steel and  $\frac{1}{8}$ -in. titanium on  $\frac{1}{2}$ -in. steel clads were made at two different collision velocities well inside the wavy bond range. The collision angle was varied over a considerable range by varying the stand-off. The bond zones of the clads were examined metallographically and the wave size (amplitude) was measured in each case. Fig. 7 shows a plot of bond zone wave amplitude versus the square of the collision angle. The wave amplitude is strongly dependent on collision angle and independent of collision velocity.

Burkhardt, Hornbogen, and Keller<sup>13</sup> and Deribas, Kudinov, and Matveenkov,<sup>20</sup> also observed a transition from a smooth to a wavy bond zone at a critical collision velocity independent of collision angle. On the other hand, Bahrani and Crossland<sup>5</sup> reported a transition from a wavy bond zone to a smooth bond zone with increasing collision angle. This can be accounted for by the fact that in their experiments made with a curved backer, the collision velocities were decreasing as the collision angle was increasing; the critical boundary line crossed in their experiments might well have been independent of collision angle.

#### The Fluid Flow Analogy

The striking similarity between the flow patterns observed at different Reynolds numbers in fluid flow past an obstacle and the configuration of the bond zones in clads made at different velocities may be seen by comparing Figs. 4 to 6 with Fig. 8 showing photographs of the flow patterns in oil behind circular transverse cylinders.<sup>17,21,27</sup> There is a transition from smooth flow at  $R = 32$  to an oscillating wake at  $R = 55$ , with a well-developed von Karman vortex street and vortex shedding showing up at higher values of  $R$ . The configuration of the wavy bond zone appears to be the frozen pattern of the plastic metal flow. Pockets of solidified metal occur at the vortices where plastic deformation is most severe and the associated heating causes localized melting. Near the transition line where even localized melting is very slight or does not occur, the configuration obtained, even though similar to that obtained for fluids, results from plastic deformation of the solid metals. This, coupled with the fact noted above that the transition at values of  $\theta$  of interest is substantially independent of  $\theta$ , suggests that the Reynolds number for cladding,  $R_c$ , should be formulated in terms of the static strength of the metals. Defining  $R_c$  as the ratio of the maximum inertial stress to the actual stress resisting deformation, we take the maximum inertial

Table I. "Reynolds Numbers" for Different Cladding Systems at Transition from Straight to Wavy Bond Zones

Symmetric Systems								
System	Density, g per cu cm	Hardness		Observed Collision Velocity at Transition cm per sec	Reynolds Number at Transition $R_T = \frac{(\rho_p + \rho_B)V_T^2}{2(H_p + H_B)}$			
		Dphn kg per sq mm	Dyne per sq cm					
Mg/Mg ZE10A	1.74	46	$45 \times 10^8$	$2.50 \times 10^5$	12.0			
Al/Al 6061T6	2.7	82	$80 \times 10^8$	$2.30 \times 10^5$	8.9			
Al/Al 1100H14	2.7	49	$48 \times 10^8$	$1.9 \times 10^5$	10.1			
Ti/Ti 35A	4.54	120	$118 \times 10^8$	$2.39 \times 10^5$	11.0			
Fe/Fe A-212 Steel	7.86	118	$116 \times 10^8$	$1.96 \times 10^5$	13.0			
Fe/Fe 1008 Steel	7.86	101	$100 \times 10^8$	$1.80 \times 10^5$	12.8			
Ni/Ni "A"	8.9	133	$130 \times 10^8$	$\sim 1.60 \times 10^5$	$\sim 8.7$			

Asymmetric Systems								
System	Density g per cu cm		Hardness		Observed Collision Velocity at Transition cm per sec	Reynolds Number at Transition $R_T = \frac{(\rho_p + \rho_B)V_T^2}{2(H_p + H_B)}$		
	Prime	Backer	Dphn	Prime dyne per sq cm			Dphn	Backer dyne per sq cm
DLP Cu/1100H14 Al	8.90	2.70	66.5	$64.3 \times 10^8$	49	$48.1 \times 10^8$	$\sim 1.6 \times 10^5$	$\sim 13.1$
35A Ti/1008 Steel	4.54	7.87	120	$118 \times 10^8$	101	$99.2 \times 10^8$	$\sim 1.75 \times 10^5$	$\sim 8.7$
"A" Ni/1008 Steel	8.9	7.87	133	$131 \times 10^8$	101	$99.2 \times 10^8$	$\sim 1.75 \times 10^5$	$\sim 10.5$
35A Ti/5051T6 Al	4.54	2.70	120	$118 \times 10^8$	82	$80.5 \times 10^8$	$\sim 2.1 \times 10^5$	$\sim 8.1$

Observed Average  $R_T = 10.6$   
 Observed Relative Standard Deviation - 17.9%

stress as the stagnation pressure of the flow in the steady-state coordinate system moving with the collision, and approximate this by the expression for incompressible flow, since the effect of compressibility is generally negligible. As a measure of the static

strength we use the diamond pyramid hardness, since it includes the effect of work hardening, and is simple to determine. In metal cladding the prime metal and the backer metal are usually different materials; to

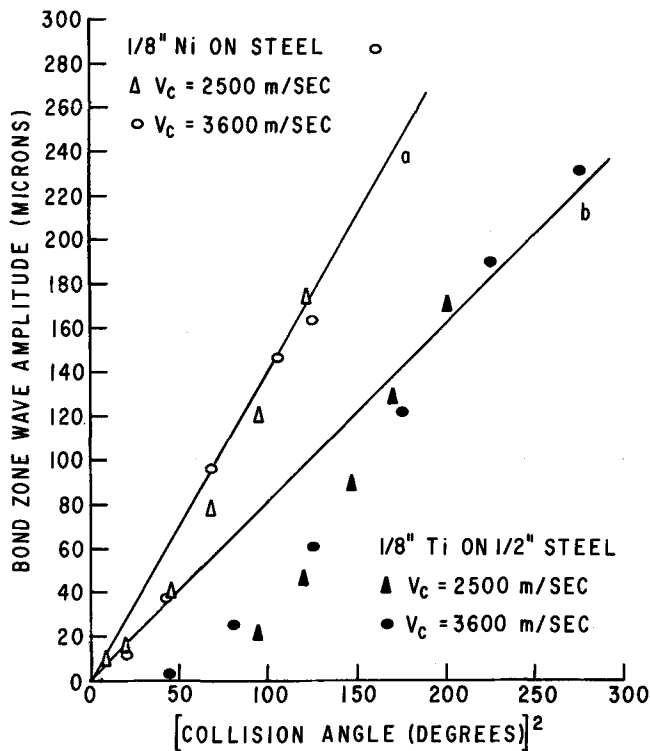


Fig. 7—Influence of collision angle on bond zone wave amplitude for nickel/steel and titanium/steel made at different collision velocities. Lines a and b are based on the fluid flow analogy.

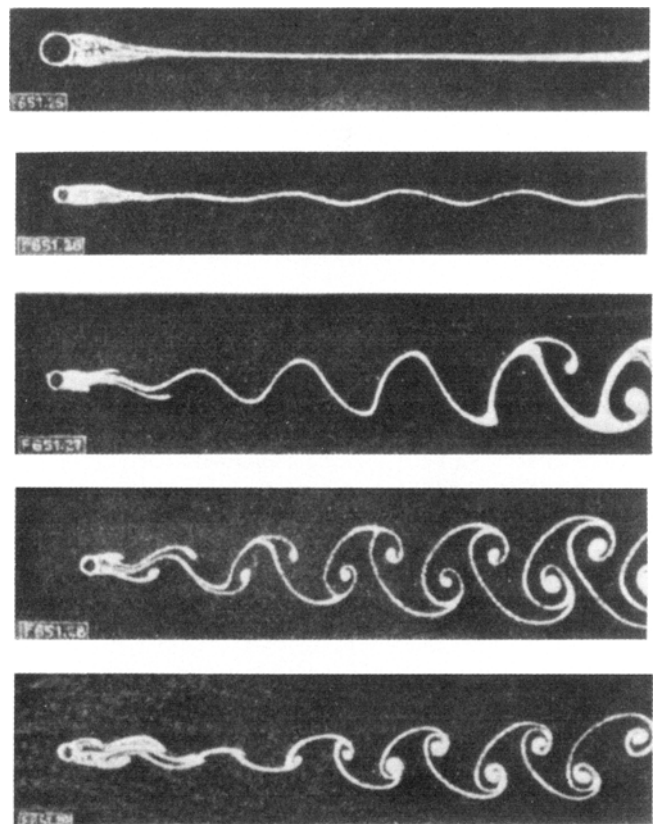


Fig. 8—Photographs of fluid flow behind cylinders at increasing values of the Reynolds number,  $R$ , after F. Homann.<sup>27</sup>

allow for this we use average values for the density and hardness. The Reynolds number for cladding then becomes:

$$R_c = \frac{(\rho_p + \rho_b)V_c^2}{2(H_p + H_b)} \quad [7]$$

where

$\rho_p, \rho_b$  = densities of prime and backer metals, g per cu cm

$V_c$  = collision velocity, cm per sec

$H_p, H_b$  = diamond pyramid hardness of prime and backer metals, dyne per sq cm =  $0.981 (\text{Dph}) \times 10^{10}$

If Eq. [7] is a valid expression for the Reynolds number for cladding, transition from a straight bond zone to a wavy bond zone should occur in different clad systems at about the same critical value of the Reynolds number,  $R_T$ , associated in general with different values of the collision velocity at which the transition occurs,  $V_T$ .

$$R_T = \frac{(\rho_p + \rho_b)V_T^2}{2(H_p + H_b)} \quad [8]$$

Values of  $R_T$  for a number of symmetric and asymmetric metal systems were calculated from the experimentally observed transition velocities and the results are shown in Table I. It is seen that transition from a smooth to a wavy bond zone occurs at nearly the same  $R_T$  values for all systems in spite of the fact that the density ranged from 1.74 g per cu cm for magnesium to 8.9 for nickel and the hardness ranged from about Dph 50 to Dph 133. The average of the experimentally observed  $R_T$  numbers in Table I is 10.6 having a relative standard deviation of 17.9 pct.

An estimate was made of the overall standard experimental error expected for  $R_T$  from the estimated errors of the individual quantities used in computing  $R_T$ . The records of the experimental data indicated the following estimated relative errors: density—0.2 pct, hardness—4.0 pct, collision velocity at transition—8.0 pct. Standard procedures for calculation of error propagation gave an expected overall experimental error of 16.5 pct for  $R_T$ . It is seen that the observed relative standard deviation from 11 different series of experiments is only slightly larger than the expected relative standard error. Furthermore, all observed  $R_T$  values of Table I are within the 95 pct confidence limit prescribed for a normal distribution to be within  $\pm 2$  standard errors of the average. The results given above therefore indicate strongly that  $R_T$  is indeed a constant. However, there is a possibility that the critical Reynolds number for different classes of metals may vary somewhat (due to differences in strain rate dependent strength properties) but these effects are not large compared with the present experimental error. Some variation in  $R_T$  may also be expected from the fact that hardness is not a precise measure of the resisting stresses under the conditions of bond zone formation. The best estimate of the value of  $R_T$  is 10.6 with a standard relative error of 17.9 pct. The finding that  $R_T$  is substantially a constant for different metal sys-

tems in explosion cladding represents very strong support for the validity of the fluid-flow analogy theory of bond zone wave formation.

Our second objective is to account for the size of the waves in cladding, the strong dependence of size on collision angle, and its independence of collision velocity, on the basis of the analogy to the vortex streets in fluid flow past obstacles. As noted in the introduction, the problem is complicated by differences in geometry and material properties and by the lack of simple theoretical solutions for liquids. Nevertheless we attempt an absolute correlation in spite of the numerical uncertainty.

The size of the vortex street in fluid flow is usually described in terms of the dimensionless Strouhal number  $S = Nd/V_c$ <sup>16</sup> where  $N$  is the frequency,  $d$  is a characteristic dimension of the obstacle, and  $V_c$  is the upstream velocity. For different obstacles the experimental values of the Strouhal number, based on some arbitrary characteristic dimension of the obstacle, differ to some extent, though not greatly. Attempts to define a universal Strouhal number have been only partly successful, being deficient in accuracy or generality. Most of these are based on relating the Strouhal number to the width of the wake created by the obstacle. Goldberg, Washburn, and Florsheim<sup>22</sup> suggest the total wake momentum thickness,  $\delta_m$ , which may be defined in terms of the drag,  $E_d$  per unit transverse length, on an obstacle of width  $d$  moving with velocity  $V_c$ , through a medium of density  $\rho$ ,

$$\rho V_c^2 \delta_m = E_d = \rho V_c^2 C_D d/2 \quad [9]$$

$$\delta_m = (C_D/2)d \quad [10]$$

$C_D$  is the drag coefficient.

Strouhal numbers based on  $\delta_m$  still show some variability, which can be attributed to different velocity profiles across the wake. If we use an average wake velocity  $\alpha V_c$  corresponding to an obstacle velocity  $V_c$ , we obtain a wake width  $\delta$  from

$$E_d = \rho V_c \alpha V_c = \rho V_c^2 C_D d/2 \quad [11]$$

$$\delta = (C_D/2\alpha)d = E_d/\rho \alpha V_c^2 \quad [12]$$

In the wavy bond zone the vortex street is frozen in, so that the wavelength  $\lambda$  is given simply as

$$\lambda = V_c/N = d/S = \delta/S_\delta \quad [13]$$

where  $S_\delta$  is a "universal" Strouhal number based on the wake width  $\delta$ . For waves of a given shape the amplitude  $a$  may be expressed as

$$a = g\lambda = g\delta/S_\delta = 2gE_d/SC_D V_c^2 = gE_d/S_\delta \alpha \rho V_c^2 \quad [14]$$

The energy dissipated in the collision  $E$  can be obtained from the conservation of momentum by neglecting the momentum of the jet, which is extremely small for low collision angles. The resulting expression is<sup>1</sup>

$$E = bm_p V_p^2/2 \quad [15]$$

where  $b = m_b/(m_p + m_b)$ . In the absence of friction, this energy would constitute the kinetic energy of an ideal jet with velocity  $2V_c$ . The mass  $m_j$  per unit area of this ideal jet can be obtained in terms of  $\theta$  by using Eq. [1].

$$m_j = (bm_p/2) \sin^2(\theta/2) \cong bm_p\theta^2/8 \quad [16]$$

In the actual case, only part of this energy is carried off by the jet with the remaining fraction  $KE$  constituting the energy of the wake flow, analogous to the drag energy per unit length of travel of an obstacle in fluid flow. Bergmann, Cowan, and Holtzman<sup>11</sup> measured a value  $K = 0.3$  for a nickel-to-steel cladding shot with  $V_c = 4750$  m per sec. Measurements of melted layer thickness given by Cowan and Holtzman<sup>1</sup> on stainless steel to steel clads with  $V_c = 3900$  m per sec indicate  $K$  values of about 0.5. Since oscillation occurs in the collision region itself, it is possible that the jet energy contributes to generation of the vortex street. The effective value of  $K$  is thus somewhat uncertain, but probably lies between 0.3 and 1. The expression for the wave amplitude becomes

$$\begin{aligned} a &= gKbm_p V_p^2 / 2\alpha S_\delta \rho V_c^2 \\ a &= (2gKbm_p / \alpha S_\delta \rho) \sin^2(\theta/2) \\ &= (gKbm_p / 2\alpha S_\delta \rho) \theta^2 \text{ for small } \theta \end{aligned} \quad [17]$$

Values of  $\alpha S_\delta$  ( $= SC_D/2$ ) will be obtained from fluid flow around a transverse circular cylinder and around a flat plate. The study by Taneda<sup>23</sup> of the oscillation of the wake behind a flat plate parallel to the flow is of considerable interest because the oscillating wake and vortex street arise from a laminar wake rather than from the separated flow around a bluff body. The straight bond zone configuration obtained below the critical collision velocity is more like that expected from freezing in a laminar wake than a separated wake. Taneda found the wake completely smooth below a Reynolds number  $R_L = 700$ , based on the length of the flat plate, with a regular oscillation above  $R_L = 1000$ , and vortices at still higher values of  $R_L$ . Over the range of his measurements from  $R_L = 2000$  to 80,000 Taneda found that  $S$  was proportional to  $R_L^{1/2}$ . Evaluating the constant from Taneda's Fig. 5, we obtain

$$S = 0.048 R_L^{1/2} \quad [18]$$

On the other hand the drag coefficient is known from boundary layer theory<sup>24</sup>

$$C_D = 2.656 R_L^{-1/2} \quad [19]$$

Thus

$$SC_D/2 = 0.064 \quad [20]$$

and is independent of Reynolds number.

For the transverse circular cylinder both  $S$  and  $C_D$  are almost independent of Reynolds number above  $R = 300$ , up to the transition to a turbulent boundary layer at extremely high values of  $R$ . Below  $R = 300$ ,  $S$  decreases and  $C_D$  increases. From values of  $C_D$  from Perry's Handbook<sup>25</sup> and Roshko's empirical expression for  $S$ <sup>26</sup>,  $SC_D/2$  varies from about 0.103 to 0.123 to 0.106 for  $R$  from 60 to 300 to 1000; an average value of 0.12 will be used.

The difference between the two values of  $SC_D/2$  ( $= S_\delta\alpha$ ) is not unexpected in view of the large difference in velocity profile across the wake. For the known nearly triangular velocity profile for the laminar wake from the flat plate we arbitrarily set  $\alpha = 0.5$  as a reasonable value. To obtain identical

values of  $S$  would require  $\alpha = 0.94$  for the separated wake behind a circular cylinder.

We are now in position to determine if Eq. [17] can be used to fit the experimental wave amplitude data, shown in Fig. 7, with reasonable values for the parameters. Consider first the nickel/steel clads, where the difference in densities is small. The wave configuration in this case is quite symmetrical, and the wave shape as measured by  $g = a/\lambda$  appears to be similar to that observed in fluids. For the nickel/steel clads  $g$  has a nearly constant value of 0.20, decreasing some at small angles, except close to the transition, where it decreases considerably, as is observed in fluids. Using an average density of 8.36 per cu cm for  $\rho$  in Eq. [17], and inserting  $m_p = 2.81$  g per sq cm and  $b = 0.78$ , and changing units so that  $a$  is in microns and  $\theta$  is in degrees, we obtain

$$a = 0.08 (K/\alpha S_\delta) \theta^2 \quad [21]$$

From the slope of the straight line shown in Fig. 7 we obtain  $S_\delta\alpha/K = 0.057$ , or for  $K = 0.3, 1.0, \alpha S_\delta = 0.017, 0.057$ , and for  $S_\delta = 0.128, \alpha = 0.134, 0.45$ . If the effective value of  $K$  is indeed about 1, the vortex street configuration is closely similar to that in the wake of a flat plate ( $\alpha S_\delta = 0.064$ ). If  $K$  is somewhat less than 1 the value of  $\alpha S_\delta$  in cladding is still plausible in view of the difference between the values for a circular cylinder and a flat plate.

Eq. [17] predicts that the wave amplitude is independent of collision velocity  $V_c$ , as was found experimentally. The predicted  $\theta^2$  dependence on collision angle is also quite good. There is a slight trend for the experimental values of amplitude to fall below the curve at lower values of  $\theta$ . Part of this can be attributed to a change in wave shape, *i.e.*, a decrease in  $g = a/\lambda$  with decreasing  $\theta$ , that occurs as the boundary line for oscillation is approached. Thus it is apparent that the formation of the wavy bond zone in cladding is basically similar to the development of a von Karman vortex street behind an obstacle, in particular a flat plate, moving with constant velocity through a fluid, with the wake flow however having its origin in the geometry of the oblique collision.

The straight line  $b$  in Fig. 7 was computed for the titanium/steel clads using appropriate values of  $m_p, b$ , and average density for  $\rho$  ( $= 6.18$  g per cu cm), the same value of  $K/\alpha S_\delta$  as used for the nickel/steel clads, and a value  $g = 0.15$  which is the average for the top five experimental points. It may be noted in Fig. 3 that in this rather asymmetric system (densities of 4.5 g per cu cm for titanium vs 7.86 g per cu cm for steel) the wave shape is asymmetric and the waves are flatter than in the symmetric systems. Furthermore  $g$  decreases more strongly with decreasing angle. It is clear from Fig. 2 that at high values of  $\theta$  the wave size is in agreement with that predicted from the fluid wake flow, but at low values of  $\theta$  the asymmetry appears to have a stabilizing influence that represses the oscillating motion.

## LIQUID STREAM EXPERIMENTS

If the wave formation in cladding is in fact analogous to the generation of oscillating wakes in fluid flow, then one would expect that a transition from smooth to oscil-



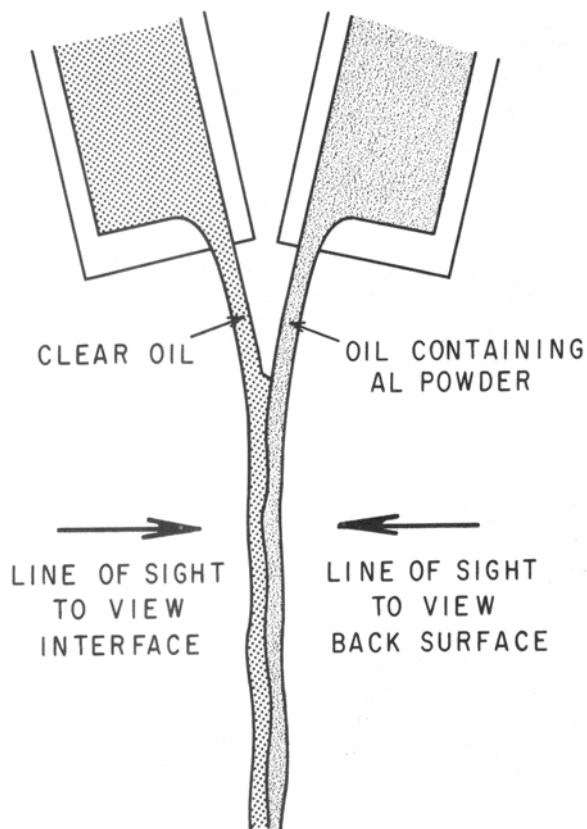


Fig. 9—Schematic plan of the experimental arrangement used to study oscillations in colliding liquid streams.

lating behavior should be observable in colliding flat liquid streams. To our knowledge no such observations have been reported. A number of experiments were carried out with flat liquid streams colliding at small to moderate angles similar to those used in cladding. A workable range of velocities and volumetric flow rates that would bracket the transition and give observable wave sizes, and would also minimize the disturbing effect of surface tension, was selected using a Reynolds number  $R_\delta$  based on the wake mo-

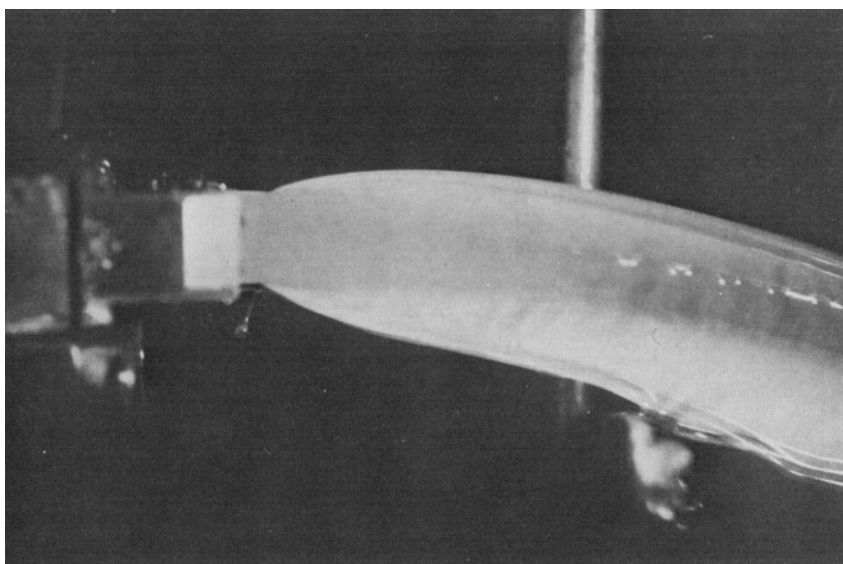
mentum width  $\delta$ , with a critical value similar to those observed for flow past obstacles, *i.e.*, about 50. The arrangement used is shown schematically in Fig. 9. Two rectangular streams from two vertical rectangular contoured half-nozzles were directed horizontally against each other at known adjustable angles. The stream velocities were adjustable up to about 900 cm per sec. The nature of the interface between the streams was observed visually using a short-duration stroboscopic light, and single flash shots were recorded with a camera. It was found that the interface could be observed with virtually identical liquids by using clear oil for the front stream and adding a very small amount of aluminum flake powder to the rear oil stream to provide contrast. With equal stream velocities a virtually symmetric collision could be obtained and interfacial surface tension eliminated. At low stream velocities a smooth interface was obtained as shown in the photograph of Fig. 10. Upon increase of the stream velocity to a higher value, the interface began to oscillate and showed a very regular wave pattern shown in Fig. 11. Because of the absence of confining walls at the top and bottom of the collision region, extensive but very thin plumes were created by the pressure in the collision region. However the rate of penetration of disturbances into the central two dimensional region is relatively slow, as is apparent from Fig. 10. At large collision angles, 22 deg in Fig. 10, the amplitude of the oscillation grows to engulf the full width of the combined stream. It can be seen clearly in Fig. 10 that the oscillation originates at the interface, and this was confirmed by photographing the rear opaque stream.

If the waves are assumed to be carried along at approximately the mainstream velocity well downstream from the collision line, the wavelength  $\lambda$  can be related to the Strouhal number in the same way as was done for the cladding experiments. Rearranging Eq. [17]

$$\alpha S_\delta / K = b W_p \theta^2 / 2\lambda \quad [22]$$

where  $W_p$  is the thickness of each incoming stream. For the values obtained from the experiment in Fig. 10, *viz.*,  $\theta = 22 \text{ deg} = 0.382 \text{ radians}$ ,  $W_p = 0.2 \text{ in.}$ ,  $\lambda = 0.31 \text{ in.}$ ,  $b = 0.5$ , then  $\alpha S_\delta / K = 0.024$ , which may

Fig. 10—Liquid stream collision (oil/oil) at low collision velocity—smooth interface.  $V_c = 168 \text{ cm per sec.}$   $\theta = 22 \text{ deg.}$



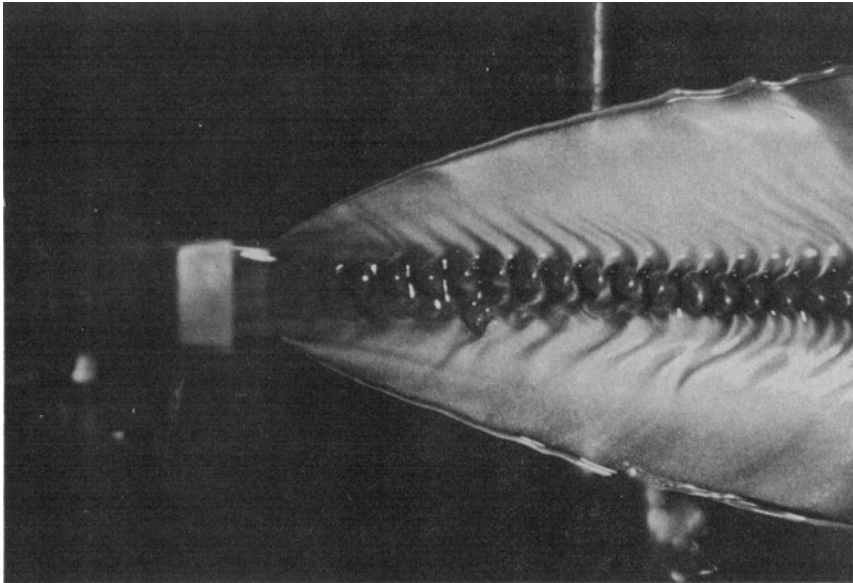


Fig. 11—Liquid stream collision (oil/oil) at higher collision velocity—wavy interface.  $V_C = 500$  cm per sec.  $\theta = 22$  deg.

be compared to the value 0.057 obtained for the nickel/steel clads. If  $K = 1$ ,  $\alpha S_\delta = 0.024$ , compared to the value 0.064 for the wake from a flat plate. Setting  $S_\delta = 0.128$  as a universal Strouhal number, so that  $\alpha = 0.18$ , we can obtain a wake momentum width  $\delta$ , on which a Reynolds number  $R_\delta = \delta V_C \rho / \mu$  can be based.

$$\delta = \lambda S_\delta = K b W_p \theta^2 / \alpha = 2.73 b W_p \theta^2$$

$$R_\delta = 2.73 b m_p \theta^2 V_C / \mu$$

For  $b = 0.5$ ,  $m_p = 0.457$  g per sq cm,  $\mu = 0.5$  poise,

$$R_\delta = 1.25 \theta^2 V_C$$

Three points on the critical boundary were closely located in the course of the experiments:  $\theta = 14$  deg,  $V_C = 840$  cm per sec,  $R_\delta = 63$ ;  $\theta = 18$  deg,  $V_C = 500$  cm per sec,  $R_\delta = 62$ ;  $\theta = 20$  deg,  $V_C = 425$  cm per sec,  $R_\delta = 65$ . For the flat plate, we have

$$R_\delta = (\delta/L) R_L = (C_D/2\alpha) R_L \quad [23]$$

For

$$\alpha = 0.5, R_\delta = C_D R_L = 2.656 R_L^{1/2}$$

According to Taneda, the critical value of  $R_L$  at which wake oscillation begins is about  $R_L = 700$ , giving  $R_\delta = 70$ .

The fact that  $\alpha S_\delta$  is less for the colliding liquid streams than for the flow past a flat plate may indicate that  $S_\delta$  is less for the colliding streams. The absence of a fixed object in the colliding streams may allow larger oscillations. The difference between the values of  $\alpha S_\delta$  for colliding liquid streams and the collision of metal plates in cladding presumably reflects the difference in material properties, and in particular the stabilizing effect of the finite yield strength of the metals surrounding the oscillating region.

#### Alternate Wave Formation Mechanisms

It was of considerable interest to examine the applicability of alternate mechanisms of wave formation in explosion bonding of metals. The possibility was ex-

plored that either a) elastic vibrations, produced in the prime metal during cladding, or b) that the "hot wind" that precedes the collision front and which consists of a mixture of jet and highly compressed air, might be responsible for bond zone wave formation.

A number of special cladding experiments were designed and carried out to determine whether or not a causal relationship exists between the size of harmonic elastic vibrations in the prime metal and the size of the bond zone waves found in explosion clads. The results of these experiments showed that such vibrations have no influence on the formation or the size of the bond zone waves and this mechanism can therefore be ruled out.

In the "hot wind" theory waves are thought to be formed by the hot mixture of jet and highly compressed air that precedes the collision front. This mixture was thought to heat up the metal surfaces sufficiently to cause melting of the surface and the "hot wind" would then cause ripples in much the same manner as wind blowing over a body of stagnant water. This theory was explored in a special cladding experiment in which the downstream end (the last 15 pct) of the cladding assembly was not covered with explosive. The purpose of this arrangement was to determine whether or not wave formation continued beyond the downstream end of the explosive layer. If the "hot wind" theory was valid, wave formation would be expected to continue for a considerable distance beyond the end of the explosive layer because this part would be exposed to the action of jet and hot air for some time in spite of the fact that this part of the plate was not driven by the detonation. Exposure to jet and compressed air in this part is caused by the fact that the jet and the hot air associated with it have a velocity of about 1.5 times detonation velocity when cladding is carried out in air.<sup>11</sup> Careful visual as well as metallographic examination of the clad after the shot showed that beyond the region covered by the explosive charge there were no signs of waves in the metals and bonding between the metals also stopped at the transition line. These results show

clearly that the "hot wind" (egressing jet and compressed air preceding the collision front) cannot be responsible for the observed bond zone waves. These results also showed definitely that wave formation in the bond zone is intimately associated with the high-velocity collision between the plates. The evidence is consistent with the fluid-flow analogy mechanism, but inconsistent with the "hot wind" or the elastic vibration mechanism.

### CONCLUSIONS

The quantitative measurements obtained from cladding experiments carried out with well-defined values of the collision variables indicate that the formation of the wavy bond zone in explosion cladding is analogous to the formation of an oscillating wake and vortex street in fluid flow past an obstacle. The transition from a smooth to a wavy bond zone with increasing collision velocity can be predicted quantitatively from a universal critical value of a Reynolds number defined in terms of average density and hardness of the two metals. The dependence of wave size on collision angle can be accounted for by the analogy between the energy dissipated in cladding and the energy dissipated by drag. Substantially quantitative agreement with the observed flow past a flat plate at zero incidence is obtained when all of the dissipated energy, including that carried off as kinetic energy of the escaping jet, is taken as contributing to the wave formation. Experiments with colliding flat liquid streams, in which a transition from smooth to oscillating behavior was observed, support the analogy.

### ACKNOWLEDGMENTS

We thank A. B. Ashenfelter for much of the laboratory work, W. Simmons for carrying out most of the liquid stream experiments, and J. Bonner as well as D. Thomas for their photographic skills. Thanks are due to C. O. Davis, M. S. Brinn, D. L. Coursen, H. F. Ring, and W. A. Jenkins for their interest and en-

couragement. The Du Pont Company's permission to publish this report is gratefully acknowledged.

### REFERENCES

1. G. R. Cowan and A. H. Holtzman: *J. Appl. Phys.*, 1963, vol. 34, pp. 328-39.
2. A. H. Holtzman and G. R. Cowan: *Welding Research Council Bulletin* No. 104, April, 1965, American Welding Society, New York.
3. U.S. Patent 3,137,937.
4. U.S. Patent 3,233,312.
5. A. S. Bahrani and B. Crossland: *Proc. Inst. Mech. Eng.*, 1965, vol. 179, p. 264.
6. A. S. Bahrani and B. Crossland: *Proc. Inst. Mech. Eng.*, 1965-66, vol. 180, Part 31, Paper 22.
7. E. Schmidtman, W. Koch and H. Schenk: *Arch. Eisenhüttenw.*, 1965, vol. 36, pp. 667-76.
8. B. Crossland, A. S. Bahrani, J. D. Williams, and V. Shribman: *Welding and Material Fabrication*, 1967, vol. 35, pp. 88-94.
9. J. L. Demaris and A. Pocalyko: *Am. Soc. of Tool Manuf. Eng.*, 1966, ASTM Paper AD66-113.
10. A. Pocalyko and C. P. Williams: *Welding J.*, 1964, vol. 43, pp. 854-61.
11. O. R. Bergmann, G. R. Cowan and A. H. Holtzman: *Trans. TMS-AIME*, 1966, vol. 236, pp. 646-53.
12. W. Klein: *Techn. Mitt Krupp Forsch. Ber.*, 1965, vol. 23, pp. 1-9.
13. A. Burkhardt, E. Hornbogen and K. Keller: *Z. Metallk.*, 1967, vol. 58, pp. 410-15.
14. O. R. Bergmann: *Met. Eng. Quart., ASM*, 1966, pp. 60-64.
15. A. S. Bahrani, T. J. Black, and B. Crossland: *Proc. Roy. Soc.*, 1967, vol. A296, pp. 123-36.
16. G. Birkhoff and E. H. Zarantello: *Jets, Wakes, and Cavities*, p. 280, Academic Press, New York, 1957.
17. *Modern Developments in Fluid Dynamics*, S. Goldstein, ed., Dover Publications, Inc., New York, 1965.
18. F. H. Harlow and J. E. Fromm: *Phys. Fluids*, 1964, vol. 7, pp. 1147-56.
19. G. R. Cowan and A. S. Balchan: *Phys. Fluids*, 1965, vol. 8, pp. 1817-27.
20. A. A. Deribas, V. M. Kudinov, and F. I. Matveenkov: *FGV [Combustion, Explosions and Shock Waves]*, 1967, vol. 3, pp. 561-68 [344-48].
21. L. Prandtl: *Essentials in Fluid Dynamics*, Haffner Publishing Co., New York, 1944.
22. A. Goldburg, W. K. Washburn, and B. H. Florsheim: *AIAA Jour.*, 1965, vol. 3, pp. 1332-33.
23. S. Taneda: *J. Phys. Soc. Japan*, 1958, vol. 13, pp. 418-25.
24. *Modern Developments in Fluid Dynamics*, S. Goldstein, ed., p. 136, Dover Publications, Inc., New York, 1965.
25. *Chemical Engineers' Handbook*, 4th Ed., J. H. Perry, ed., p. 5-60, McGraw-Hill, Inc., New York, 1963.
26. R. Wille: in *Advan. Appl. Mech.*, vol. VI, p. 281, Academic Press, New York, 1960.
27. Homann, F.: *Forsch. Gebiete Ingenieurw.*, 1936, vol. 7, pp. 1-10.